Field-oriented Control of an Induction Machine with Winding Asymmetries

Vinko Lešić[1)], Mario Vašak[1)], Marko Gulin[1)], Nedjeljko Perić[1)], Gojko Joksimović[2)] and Thomas M. Wolbank[3)]
[1)]University of Zagreb, Faculty of Electrical Engineering and Computing, Zagreb, Croatia
[2)]University of Montenegro, Faculty of Electrical Engineering, Podgorica, Montenegro
[3)]Vienna University of Technology, Faculty of Electrical Engineering and Information Technology, Vienna, Austria
vinko.lesic@fer.hr, mario.vasak@fer.hr, marko.gulin@fer.hr, nedjeljko.peric@fer.hr, joxo@ac.me, thomas.wolbank@tuwien.ac.at

***Abstract*—Modern electrical AC drives with best available performances are based on the so-called fundamental wave machine model approaches. This paper introduces an upgrade of fundamental wave model approach by respecting both inherent and fault-induced deviations of machine flux from its fundamental component. A field-oriented control scheme for an asymmetric induction machine is presented. The algorithm is based on observing newly introduced flux-angle-based variations in the transient leakage inductance due to the asymmetry. A simple extension of the conventional rotor field-oriented control structure is proposed that takes into account detected variations and improves machine performance in the asymmetry conditions. Detection and characterization of newly formed modulation in transient leakage inductance are performed by employing an unscented Kalman filter. Simulation results for the case of a 5.5 kW induction machine are presented.**

***Index Terms*—Asymmetric Induction Machine, Field-oriented Control, Dual Unscented Kalman Filter.**

I. Introduction

Increasing demands for dynamic performances of electrical drives led to the fact that field-oriented control (FOC) or direct torque control (DTC) have been adopted as standard control strategies in widely-spread industrial applications for last 15 years [1]. Both of them belong to the group of control methods that use the so-called fundamental wave machine model. The fundamental wave approach is a generally accepted method for modeling the machine flux position, which assumes ideal and sinusoidal flux distribution in the machine air gap, i.e. neglects saliencies, saturation, hysteresis losses and other nonlinearities and asymmetries due to machine physics and geometry.

Our motivation for respecting asymmetries in the machine operation arose from observing wind turbine generator electromechanical faults and providing the corresponding fault-tolerant control. Building on the fault detection algorithm [2][3], fault-tolerant control should provide an autonomous reaction in order to suppress the fault spreading and to enable smooth operation of the generator. Rotor-bar and stator winding inter-turn faults of a squirrel-cage induction machine are considered. Occurred faults introduce more or less asymmetries in the machine operation and cause degradation of the wind turbine performance.

If a short-circuit occurs in a stator winding, the shorted turn (or few of them) is segregated from the healthy machine phase. The shorted turn can be observed as a newly formed phase in the machine with its own resistance and inductance [4]. This new phase is also influenced by the variable magnetic flux that induces voltage and introduces a current flow in the shorted turn. Consequences are machine local overheating and undesired torque modulation around the reference value.

In this paper, more general and, from the control viewpoint, more convenient approach for representation of the asymmetry is considered. The approach is relied on detecting changes in transient leakage inductance due to the inherent asymmetry, the occurred fault [2][3], or both. Depending on the detection capability and by assuming the machine can operate safely in asymmetric conditions, the proposed algorithm can be applied regardless of the asymmetry cause. In the sequel, the stator winding inter-turn short circuit is considered.

In [5], a method for suppressing the stator inter-turn short-circuit by modulating the fundamental magnetic flux and thereby restricting the current flow in the shorted-turn is proposed. This allows the machine to operate safely under fault condition without local overheating.

The focus here is to improve the drive control performance in terms of FOC algorithm upgrade to overcome the asymmetries and corresponding torque degradation. The algorithm is conceived as an extension of widely-adopted rotor-flux-based FOC used in control of symmetric induction machines. The goal is to make the extension with minimum modifications of conventional control algorithms. The developed algorithm is intended for torque control of a squirrel-cage induction machine but can also be modified for control of any type of machine controlled by FOC.

This paper is organized as follows. In Section II a fundamental-wave model of a symmetric induction machine is described and a common model-based FOC algorithm is shortly presented. The stator winding isolation fault and modeling of asymmetries are briefly described in Section III. An extension of the FOC algorithm that considers machine asymmetries is proposed in Section IV, together with a procedure for asymmetry detection. Section V provides simulation results

978-1-4673-1972-0/12/$31.00 ©2012 IEEE

for the case of a 5.5 kW squirrel-cage induction machine. Conclusions are drawn in Section VI.

II. MATHEMATICAL MODEL OF AN AC MACHINE

Mathematical model of an AC squirrel-cage induction machine can be represented in the two-phase (d,q) rotating coordinate system [6][7]:

$$\bar{u}_s = R_s\bar{i}_s + \frac{d\bar{\psi}_s}{dt} + j\omega_e\bar{\psi}_s, \quad (1)$$

$$0 = R_r\bar{i}_r + \frac{d\bar{\psi}_r}{dt} + j(\omega_e-\omega_r)\bar{\psi}_r, \quad (2)$$

where bar notation represents a complex (d,q) vector, subscript s stator variables, subscript r rotor variables, i currents and R resistances. In a common rotating coordinate system stator variables are rotating with speed $\omega_e = 2\pi f$ and rotor variables with speed $\omega_e - \omega_r$, where f is the frequency of the AC voltage supplied to the stator, ω_g is the speed of rotor, $\omega_r = p\omega_g$, and p is the number of machine pole pairs. Flux linkages $\bar{\psi}_s$ and $\bar{\psi}_r$ are given by:

$$\bar{\psi}_s = L_s\bar{i}_s + L_m\bar{i}_r, \quad (3)$$

$$\bar{\psi}_r = L_m\bar{i}_s + L_r\bar{i}_r, \quad (4)$$

where $L_s = L_{s\sigma} + L_m$ is stator inductance, $L_r = L_{r\sigma} + L_m$ is rotor inductance, and L_m is mutual inductance. Parameters $L_{s\sigma}$ and $L_{r\sigma}$ are stator and rotor flux leakage inductances, respectively.

By perturbing relations (1)-(4) and by fixing the rotor flux linkage to d axis, a rotor field-oriented control (RFOC) equations are obtained:

$$i_{mr} = \frac{\psi_{rd}}{L_m}, \quad (5)$$

$$i_{sd} = i_{mr} + T_r\frac{di_{mr}}{dt}, \quad (6)$$

$$\omega_{sl} = \omega_e - \omega_r, \quad (7)$$

$$T_g = \frac{3}{2}p\frac{L_m^2}{L_r}i_{mr}i_{sq} = k_m i_{mr} i_{sq}, \quad (8)$$

where i_{mr} is the magnetizing current that creates the rotor flux, $T_r = \frac{L_r}{R_r}$ is the rotor time constant, $\omega_{sl} = \frac{i_{sq}}{T_r i_{mr}}$ is the slip speed (difference between the electrical and mechanical speed) and T_g is the electromagnetic torque. The torque is controlled only by q stator current component because magnetizing current vector i_{mr} is dependent on the time lag T_r and is therefore kept constant in the sub-nominal speed operating region.

Voltage-controlled machine (Fig. 1) is usually more suitable than the current-controlled so by eliminating ψ_s and i_r, and by introducing (5) in (1)-(4), stator voltage vector components u_{sd} and u_{sq} are obtained:

$$u_{sd} = k_s i_{sd} + L_l\frac{di_{sd}}{dt} + \left(\frac{L_l}{T_r} - \frac{L_s}{T_r}\right)i_{mr} - \omega_e L_l i_{sq}, \quad (9)$$

$$u_{sq} = R_s i_{sq} + L_l\frac{di_{sq}}{dt} - \omega_e\left(L_l - L_s\right)i_{mr} + \omega_e L_l i_{sd}, \quad (10)$$

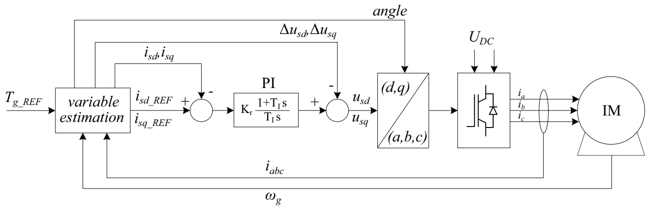

Fig. 1. Field-oriented control loop.

where $L_l = (L_s - \frac{L_m^2}{L_r})$ and $k_s = (R_s - \frac{L_l}{T_r} + \frac{L_s}{T_r})$. Parameter L_l denotes the leakage inductance. Relations (9) and (10) show that d and q coordinates are not fully decoupled and changing the voltage value in one axis, affects also the other. By introducing correction voltages Δu_{sd} and Δu_{sq}, fully decoupled relations are derived:

$$u_{sd} + \Delta u_{sd} = k_s i_{sd} + L_l\frac{di_{sd}}{dt}, \quad (11)$$

$$u_{sq} + \Delta u_{sq} = R_s i_{sq} + L_l\frac{di_{sq}}{dt}, \quad (12)$$

with

$$\Delta u_{sd} = \frac{1}{T_r}\frac{L_m^2}{L_r}i_{mr} + \omega_e L_l i_{sq}, \quad (13)$$

$$\Delta u_{sq} = -\omega_e\frac{L_m^2}{L_r}i_{mr} - \omega_e L_l i_{sd}. \quad (14)$$

These equations are now suitable for further design of the control loop and proportional-integral (PI) controllers are chosen with integral time constants $T_{Id} = L_l/k_s$ for d-current, $T_{Iq} = L_l/R_s$ for q-current and gain K_r. Finally, closed loop dynamics can now be represented as a first-order lag system with transfer function:

$$\frac{i_{sd}(s)}{i_{sd\_REF}(s)} = \frac{i_{sq}(s)}{i_{sq\_REF}(s)} = \frac{1}{1+\tau s}, \quad (15)$$

where τ is a time constant defined with $\tau = \frac{L_l}{K_r}$.

III. STATOR WINDING ISOLATION FAULT AND MACHINE ASYMMETRIES

Stator winding isolation faults represent about 30% of all machine faults [8]. They mostly appear in the stator slot (Fig. 2) due to moisture in the isolation, winding overheating, or vibrations. Modern voltage-source inverters also introduce additional voltage stress on the inter-turn isolation caused by the steep-fronted voltage surge [9][10].

Possible scenarios are short-circuit between two different machine phases, shorted turns of the same phase or phase-to-ground faults. If there is a short-circuit between two different

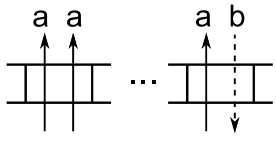

Fig. 2. Sketch of a stator slot including two turns of the same phase (aa) and two turns of different phases (ab).

phases or a phase-to-ground short circuit, the time elapsed between the fault occurrence and triggered safety device is about one third of a second. For the case of a short-circuit between turns of the same phase (stator phase inter-turn short circuit) the time elapsed between incipient fault and triggered safety device is about several minutes or even much longer, depending on the stator winding method [11]. This gives an opportunity for the fault detection and autonomous control reaction.

The stator phase inter-turn short circuit is manifested as a shorted turn in the phase winding with very low resistance. It results in high currents that flow through that turn and cause machine torque reduction and local overheating. If current in the shorted turn is kept below its rated value, the fault propagation can be stopped.

The change of stator resistances due to occurred inter-turn fault is negligible (below 1% change). The change in fundamental wave inductances is also very small (1-2% change), however, it has a noticeable effect on the instantaneous value of the transient leakage inductance. The leakage inductance comprises all fundamental wave inductances masked in a mutual product and therefore results in much greater change (up to 10%), which can be observed with a fault-detection algorithm. Shorted phase has its own resistance and inductance and affects the main flux in the machine air-gap.

Assuming the fault is suppressed and machine can operate safely, influence of the modified flux and corresponding torque modulation due to shorted turns still remains.

A. Modeling the asymmetry

For symmetric fundamental-wave machine the leakage inductance is the same for all phases and so far the parameter L_l was implied to be constant. Due to occurred asymmetry in the machine, the leakage inductance is no longer the same for all phases and can be represented with a complex value denoted with $\bar{L}_{l,t}$. It is composed of a scalar offset value L_{offset} and a complex value $\bar{L}_{mod}$. The offset value represents the symmetric part while complex value includes induced asymmetry with its magnitude and spatial direction. More about this approach can be found in [2][3]. In stator reference frame leakage inductance $L_{l,t}$ is represented as:

$$\bar{L}_{l,t} = L_{offset} + \bar{L}_{mod}, \qquad \bar{L}_{mod} = L_{mod} \cdot e^{j2\gamma}. \tag{16}$$

The angle $\gamma = \omega_e t + \varphi$ corresponds to the current location of the stator fault with respect to the magnetizing flux. The frequency is doubled due to effects of both north and south magnetic field poles per single flux revolution period.

Every machine in normal operation has inherent asymmetries, which are the result of spatial saturation, anisotropy, saliencies etc. The most conspicuous one is the saturation saliency that arises from the spatial distribution of the fundamental wave along the stator circumferences [3]. The period is also twice as of the fundamental wave. This particular inherent asymmetry is dependent on the flux magnitude and load amount and can be noticeable in normal machine operation. Another asymmetry is caused by slot openings in the rotor lamination and its period corresponds to the number of rotor bars.

For the fault detection procedure and machine diagnostics, it is important to segregate different causes of asymmetries and observe the influence of each. From the control viewpoint, the total leakage inductance is included in the control procedure as a representative value in which all contributions from different asymmetry causes are reflected, including the fault-induced ones.

IV. Control of asymmetric induction machine

In Section II a widely-adopted RFOC algorithm is described. It provides very good results and satisfying performance of a nearly symmetrical machine. Several modifications can be applied to further improve its performance. Often applied one is to consider machine saliencies by choosing different values of stator inductances in d and q axes [6]. Also a lot of effort is currently put into finding adequate solution for sensorless drives [1][13].

In the sequel, an RFOC algorithm for asymmetric machine is proposed. The algorithm is conceived as an extension of the previously described method for symmetric machine control.

By transferring to the common reference frame the leakage inductance can be represented with:

$$\bar{L}_{l,t} = L_{ld} + j \cdot L_{lq}, \tag{17}$$

where $L_{ld} = L_{offset} + L_{mod}\cos(2\gamma)$, and $L_{lq} = L_{mod}\sin(2\gamma)$.

The leakage inductance from (17) is put into induction machine stator and rotor voltage equations (1) and (2) and linear transformations of equalities are performed in the same manner as for the case of deriving conventional symmetric FOC equations. Result is the mathematical model of the asymmetric induction machine based on the variable leakage inductance approach:

$$\begin{aligned} u_{sd} =& k_a i_{sd} + L_a \frac{di_{sd}}{dt} - \frac{L_{lq}}{L_{ld}} u_{sq} + \frac{L_{lq}}{L_{ld}} R_s i_{sq} - \omega_e L_a i_{sq} + \\ & \left(\frac{L_a}{T_r} - \frac{L_s}{T_r}\right) i_{mr} + \omega_e \frac{L_{lq}}{L_{ld}} L_s i_{mr}, \end{aligned} \tag{18}$$

$$\begin{aligned} u_{sq} =& R_s i_{sq} + L_a \frac{di_{sq}}{dt} + \frac{L_{lq}}{L_{ld}} u_{sd} - \left(\frac{L_{lq}}{L_{ld}} R_s + \frac{L_{lq}}{L_{ld}} \frac{L_s}{T_r}\right) i_{sd} + \\ & \omega_e L_a i_{sd} + \frac{L_{lq}}{L_{ld}} \frac{L_s}{T_r} i_{mr} - \omega_e (L_a - L_s) i_{mr}, \end{aligned} \tag{19}$$

where $k_a = (R_s - \frac{L_a}{T_r} + \frac{L_s}{T_r})$ and $L_a = \left(L_{ld} + \frac{L_{lq}^2}{L_{ld}}\right)$. In the same way as in symmetric FOC, the decoupling method is applied. By introducing correction voltages Δu_{sd} and Δu_{sq}, fully decoupled relations are derived:

$$u_{sd} + \Delta u_{sd} = k_a i_{sd} + L_a \frac{di_{sd}}{dt}, \tag{20}$$

$$u_{sq} + \Delta u_{sq} = R_s i_{sq} + L_a \frac{di_{sq}}{dt}. \tag{21}$$

It may be observed that relations (20) and (21) have the same form as for the case of symmetric machine (11) and (12), and therefore the same controller structure can be applied. Decoupling voltages of the asymmetric machine model are:

$$\Delta u_{sd} = \frac{L_{lq}}{L_{ld}} u_{sq} - \frac{L_{lq}}{L_{ld}} R_s i_{sq} + \omega_e L_a i_{sq} - \left(\frac{L_a}{T_r} - \frac{L_s}{T_r}\right) i_{mr} - \omega_e \frac{L_{lq}}{L_{ld}} L_s i_{mr}, \quad (22)$$

$$\Delta u_{sq} = -\frac{L_{lq}}{L_{ld}} u_{sd} + \left(\frac{L_{lq}}{L_{ld}} R_s + \frac{L_{lq}}{L_{ld}} \frac{L_s}{T_r}\right) i_{sd} - \omega_e L_a i_{sd} - \frac{L_{lq}}{L_{ld}} \frac{L_s}{T_r} i_{mr} + \omega_e (L_a - L_s) i_{mr}. \quad (23)$$

Equations (18)-(23) represent the mathematical model for an asymmetric induction machine. With complex transient leakage inductance from (16) and (17), influence of the shorted phase is respected in machine control. Change of stator resistance R_s and inductance L_s due to inter-turn short-circuit is neglected as described in Section III. With $L_{ld} = L_{offset} = L_l$ and $L_{lq} = 0$ above relations are valid for symmetric machine as well and they obtain the same form as in (9)-(14).

In the same manner, PI controller parameters are chosen with integral time constants $T_{Ida} = L_a/k_a$ for d-current, $T_{Iqa} = L_a/R_s$ for q-current. Index 'a' denotes controller parameters in case of detected asymmetry. PI controller gain K_{ra} is selected with respect to the desired transient velocity and inverter constraints. Control system block scheme remains the same as in Fig. 1.

The way of detecting the true value of the leakage inductance $\bar{L}_{l,t}$ under asymmetric machine conditions determines how much the system performance is improved with the new FOC algorithm. A method of high-sensitive detection that is based on investigation of machine behavior on transient excitation caused by inverter switching is proposed in [12] and further developed in [3].

In the sequel an approach with nonlinear Kalman filter is described. The FOC algorithm is based on precisely determined flux angle, which is needed for coordinate system transformations. Control algorithm therefore includes an observer and Kalman filter is one of the common approaches. With the goal of minimum modifications to the conventional FOC control algorithm, the existing Kalman filter is extended to provide estimation of the leakage inductance. By applying this approach, the minimum computational time increase is achieved.

A. Estimation of the leakage inductance

In this paper a dual unscented Kalman filter (UKF) is used for both state and leakage inductance estimation because of its proficient ability to cope with hard nonlinearities. The UKF represents a novel approach for estimations in nonlinear systems and provides better results than extended Kalman filter (EKF) in terms of mean estimate and estimate covariance [14].

The core idea of UKF lies in unscented transformation, way of representing and propagating Gaussian random variables (GRV) through a nonlinear mapping. The unscented transformation enables better capturing of mean and covariance of GRVs than simple point-linearization of the mapping: posterior mean and covariance are accurate to the second order of the Taylor series expansion for any nonlinearity. More information about the algorithm itself and whole theory on which it relies can be found in [14].

Machine model states in common (d, q) reference frame are i_{sd} and i_{sq} stator currents, magnetizing current i_{mr} and position of the magnetic flux ρ. Mathematical model used for state estimation of the asymmetric machine via UKF is:

$$\frac{di_{sd}}{dt} = \frac{1}{L_a} u_{sd} + \frac{1}{L_a} \Delta u_{sd} - \frac{k_a}{L_a} i_{sd} + v_1, \quad (24)$$

$$\frac{di_{sq}}{dt} = \frac{1}{L_a} u_{sq} + \frac{1}{L_a} \Delta u_{sq} - \frac{R_s}{L_a} i_{sq} + v_2, \quad (25)$$

$$\frac{di_{mr}}{dt} = \frac{1}{T_r} (i_{sd} - i_{mr}) + v_3, \quad (26)$$

$$\frac{d\rho}{dt} = p\omega_g + \frac{1}{T_r} \frac{i_{sq}}{i_{mr}} + v_4, \quad (27)$$

where variables $v_{1,..,4}$ denote process noise.

For reliable estimation of i_{sd} and i_{sq} currents, the dependency on flux angle ρ has to be included in relations (24) and (25). It can be done by introducing line voltages in (a, b, c) coordinate system and by applying Park's and Clark's transform [6], which results in:

$$\begin{aligned} u_{sd} &= \tfrac{2}{3} u_{ab} \cos\rho + \left(\tfrac{1}{3}\cos\rho + \tfrac{\sqrt{3}}{3}\sin\rho\right) u_{bc}, \\ u_{sq} &= -\tfrac{2}{3} u_{ab} \sin\rho + \left(-\tfrac{1}{3}\sin\rho + \tfrac{\sqrt{3}}{3}\cos\rho\right) u_{bc}. \end{aligned} \quad (28)$$

Inputs vector for the UKF is therefore chosen to include line voltages coming out from FOC and measured generator speed:

$$u = [u_{ab} \;\; u_{bc} \;\; \omega_g]^T. \quad (29)$$

Stator currents are usually measured in electrical machine applications and they are therefore used in UKF states correction procedure. Since the state vector $x = [i_{sd} \;\; i_{sq} \;\; i_{mr} \;\; \rho]^T$ is in (d, q) coordinates and measurements are in (a, b, c) coordinates, inverse Clark's and Park's transforms are applied and measurement vector is chosen as $y = [i_a \;\; i_b]^T$:

$$\begin{aligned} i_a &= i_{sd}\cos\rho - i_{sq}\sin\rho + n_1, \\ i_b &= i_{sd}\left(-\frac{1}{2}\cos\rho + \frac{\sqrt{3}}{2}\sin\rho\right) + \\ &\quad + i_{sq}\left(\frac{1}{2}\sin\rho + \frac{\sqrt{3}}{2}\cos\rho\right) + n_2, \end{aligned} \quad (30)$$

where n_1 and n_2 denote measurement noise.

An attractive feature of UKF is that partial derivatives and Jacobian matrix (like in EKF) are not needed and continuous-time nonlinear dynamics equations are directly used in the filter, without discretization or linearization. Therefore, equations (24)-(27) and Runge-Kutta numerical integration algorithm are used for calculating predictions of states.

The UKF itself is shortly described next. The estimated state vector $\hat{x}_k$ in a discrete time-instant k is augmented to include means of process and measurement noise $\bar{v}$ and $\bar{n}$:

$$\hat{x}_k^a = \mathbb{E}(x_k^a) = \left[\hat{x}_k^T \;\; \bar{v} \;\; \bar{n}\right]^T, \tag{31}$$

where $\mathbb{E}(\cdot)$ denotes the expectation of a random variable. State covariance matrix $\mathbf{P}_k$ is also augmented accordingly:

$$\mathbf{P}_k^a = \mathbb{E}\left((x_k^a - \hat{x}_k^a)^T(x_k^a - \hat{x}_k^a)\right) = \begin{bmatrix} \mathbf{P}_k & \mathbf{0} & \mathbf{0} \\ \mathbf{0} & \mathbf{R}^v & \mathbf{0} \\ \mathbf{0} & \mathbf{0} & \mathbf{R}^n \end{bmatrix}, \tag{32}$$

where $\mathbf{R}^v$ and $\mathbf{R}^n$ are process and measurement noise covariance matrices, respectively. Time update algorithm starts with the unscented transformation and by forming the sigma points matrix $\mathcal{X}_k^a$:

$$\mathcal{X}_k^a = \left[\hat{x}_k^a \quad \hat{x}_k^a + \gamma\sqrt{\mathbf{P}_k^a} \quad \hat{x}_k^a - \gamma\sqrt{\mathbf{P}_k^a}\right]. \tag{33}$$

Variable $\sqrt{\mathbf{P}_k^a}$ is the lower-triangular Cholesky factorization of matrix $\mathbf{P}_k^a$ and $\gamma = \sqrt{L+\lambda}$ is a scaling factor. Parameter L is the dimension of augmented state x_k^a and parameter λ determines the spread of sigma points around the current estimate, calculated as:

$$\lambda = \alpha^2\left(L+\kappa\right) - L. \tag{34}$$

Parameter α is usually set to a small positive value e.g. $10^{-4} \leq \alpha \leq 1$ and κ is usually set to 1. There are $2L+1$ sigma points used for the transformation, which correspond to the columns in $\mathcal{X}_k^a = \left[(\mathcal{X}_k^x)^T \;\; (\mathcal{X}_k^v)^T \;\; (\mathcal{X}_k^n)^T\right]^T$.

Time-update equations used to calculate prediction of state $\hat{x}_{k+1}^-$ and state covariance $\mathbf{P}_{k+1}^-$ as well as prediction of output $\hat{y}_{k+1}^-$ are:

$$\begin{aligned}
\mathcal{X}_{i,k+1|k}^x &= F\left(\mathcal{X}_{i,k}^x, u_k, \mathcal{X}_{i,k}^v\right), \quad i = 0,...,2L, && (35)\\
\hat{x}_{k+1}^- &= \sum_{i=0}^{2L} W_i^{(m)} \mathcal{X}_{i,k+1|k}^x, && (36)\\
\mathbf{P}_{k+1}^- &= \sum_{i=0}^{2L} W_i^{(c)} \left(\mathcal{X}_{i,k+1|k}^x - \hat{x}_{k+1}^-\right) \times \\
&\quad \left(\mathcal{X}_{i,k+1|k}^x - \hat{x}_{k+1}^-\right)^T, && (37)\\
\mathcal{Y}_{i,k+1|k} &= H\left(\mathcal{X}_{i,k+1|k}^x, \mathcal{X}_{i,k}^n\right), \quad i = 0,...,2L, && (38)\\
\hat{y}_{k+1}^- &= \sum_{i=0}^{2L} W_i^{(m)} \mathcal{Y}_{i,k+1|k}, && (39)
\end{aligned}$$

where i is the index of columns in matrix $\mathcal{X}_k^a$ (and also in $\mathcal{X}_k^x$, $\mathcal{X}_k^v$, $\mathcal{X}_k^n$) starting from value zero. Function $F(\cdot)$ is the model vector function from (24)-(27) where the next state is obtained by Runge-Kutta numerical integration. Function $H(\cdot)$ represent measurements from (30). Weights for mean and covariance calculations are given by:

$$\begin{aligned}
W_0^{(m)} &= \tfrac{\lambda}{(L+\lambda)}, \\
W_0^{(c)} &= \tfrac{\lambda}{(L+\lambda)} + \left(1 - \alpha^2 + \beta\right), \\
W_i^{(m)} &= W_i^{(c)} = \tfrac{\lambda}{2(L+\lambda)}, \quad i = 1,...,2L.
\end{aligned} \tag{40}$$

For Gaussian distributions, $\beta = 2$ is optimal.

Measurement update algorithm is performed in the similar way as in classical Kalman filter but requires also output covariance matrix $\mathbf{P}_{\tilde{y}_{k+1}\tilde{y}_{k+1}}$ and cross-covariance matrix $\mathbf{P}_{\tilde{x}_{k+1}\tilde{y}_{k+1}}$:

$$\begin{aligned}
\mathbf{P}_{\tilde{y}_{k+1}\tilde{y}_{k+1}} &= \sum_{i=0}^{2L} W_i^{(c)} \left(\mathcal{Y}_{i,k+1|k} - \hat{y}_{k+1}^-\right) \times \\
&\quad \left(\mathcal{Y}_{i,k+1|k} - \hat{y}_{k+1}^-\right)^T, && (41)
\end{aligned}$$

$$\begin{aligned}
\mathbf{P}_{\tilde{x}_{k+1}\tilde{y}_{k+1}} &= \sum_{i=0}^{2L} W_i^{(c)} \left(\mathcal{X}_{i,k+1|k}^x - \hat{x}_{k+1}^-\right) \times \\
&\quad \left(\mathcal{Y}_{i,k+1|k} - \hat{y}_{k+1}^-\right)^T, && (42)
\end{aligned}$$

followed by the correction of predicted states and covariance:

$$\begin{aligned}
\mathbf{K}_{k+1} &= \mathbf{P}_{\tilde{x}_{k+1}\tilde{y}_{k+1}} \mathbf{P}_{\tilde{y}_{k+1}\tilde{y}_{k+1}}^{-1}, && (43)\\
\hat{x}_{k+1} &= \hat{x}_{k+1}^- + \mathbf{K}_{k+1}\left(y_{k+1} - \hat{y}_{k+1}^-\right), && (44)\\
\mathbf{P}_{k+1} &= \mathbf{P}_{k+1}^- - \mathbf{K}_{k+1}\mathbf{P}_{\tilde{y}_{k+1}\tilde{y}_{k+1}}\mathbf{K}_{k+1}^T. && (45)
\end{aligned}$$

where $\mathbf{K}_k$ is Kalman gain matrix.

At the time-instant k measurement update is executed first. It results in current estimates which may be used for the control algorithm, i.e. to obtain the current input u_k. These two parts are time-critical in the on-line implementation. They are followed by time-update algorithm part which should be finished by the next sampling instant $(k+1)$ when new measurements arrive.

For the purpose of simultaneous parameter estimation in the model (24)-(27), the UKF above is extended into so-called dual UKF. Parameters in the dual Kalman filter implementation approach are estimated with a separate filter (Fig. 3). This way two state vectors are formed: $x = [i_{sd} \;\; i_{sq} \;\; i_{mr} \;\; \rho]^T$ and $\theta = [\theta_1 \quad \theta_2]^T$, where $\theta_1 = \varphi$ and $\theta_2 = L_{mod}$, and two estimation algorithms are executed sequentially at each sampling instant. Whole control system is presented in Fig. 4. The dual Kalman filter is often referred to as a 'braided' Kalman filter in the electrical drives community.

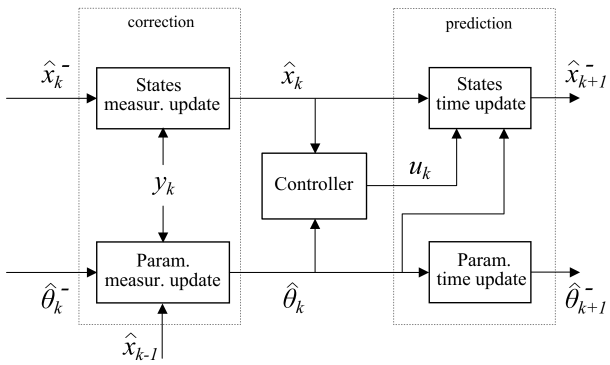

Fig. 3. Dual unscented Kalman filter scheme. Subscript 'k' represents the current time step. Hat notation is used for calculated variables and uppercase '-' is for predicted variables.

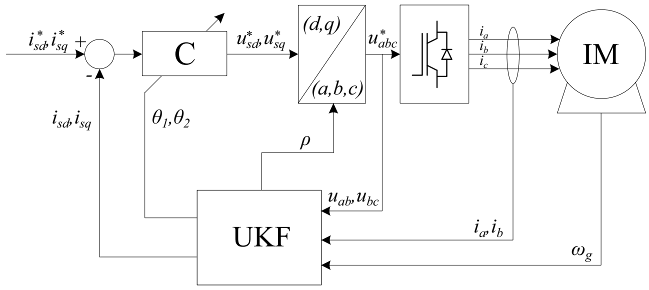

Fig. 4. Field-oriented control loop with dual unscented Kalman filter ('UKF'). Block 'C' represents the controller, block 'IM' is the squirrel-cage induction machine. Variables denoted with uppercase star '*' are referent values.

Magnetic flux rotational speed is calculated from states estimation using (7) and together with θ_1 location of the asymmetry γ in the (d, q) frame can be obtained. Considering (16) and (17), the complex value of $\bar{L}_{l,t}$ (and corresponding L_{ld} and L_{lq}) is completely determined with θ_1 (related to γ) and θ_2.

This way, only asymmetries with the period that corresponds to doubled frequency of the flux rotation are respected in operation. For this case, this refers to the stator-isolation-fault-induced asymmetry and the saturation saliency inherent one, as described in Section III.

V. Simulation results

Simulation results are obtained using MATLAB/Simulink environment and are performed on the ideal machine model. The machine considered in simulations is a four-pole squirrel-cage induction machine.

Machine parameters are: $L_s = L_r = 0.1361$ H, $L_m = 0.1308$ H, $R_s = 0.7182\ \Omega$, $R_r = 0.6047\ \Omega$ and PI controller gain for FOC is chosen $K_r = 1$. Machine rated values: stator voltage $U_n = 186.67$ V, stator current $I_n = 15.18$ A, power and torque $P_n = 5.5$ kW, $T_{gn} = 37.35$ Nm, frequency $f_n = 50$ Hz. Moment of inertia is $J = 0.02145\ \mathrm{kg \cdot m^2}$. Sample time is chosen $T_s = 2 \cdot 10^{-4}$ s.

Asymmetry is introduced as a shorted turn at location $\varphi = \pi/4$ (and $\gamma = \omega_e t + \varphi$). The leakage inductance is modified to obtain the complex form as described before with L_{mod} selected to be 10% of $L_{offset} = L_l$.

Simulations are performed with described UKF algorithm in closed loop operation with included process and measurement noises. Figures 5 and 6 are results of the same experiment.

Asymmetric machine operation is presented in Fig. 5. The machine is controlled with conventional 'symmetric' FOC ($\varphi = 0$, $L_{mod} = 0$) for first 10 s. Pulsations of machine torque and mechanical speed due to periodic characteristic of the asymmetry are evident. They are a result of inadequate decoupling procedure and poorly calculated Δu_{sd}, Δu_{sq} due to occurred asymmetry.

At time instant of 10 s, parameter estimation in UKF is enabled and parameters converge to their true values (Fig. 6). Initial values of parameters are $\theta_{10} = 0$ rad and $\theta_{20} = 0$ mH, and true values are $\theta_1 = \pi/4$ rad and $\theta_2 = 1.0327$ mH.

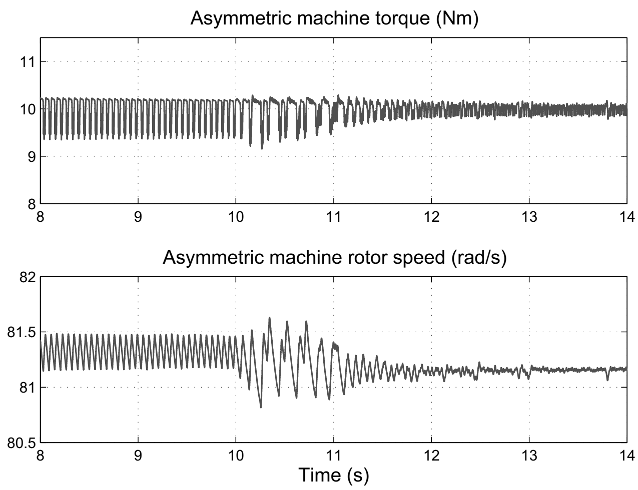

Fig. 5. Asymmetric machine torque and speed with symmetric and asymmetric FOC. Asymmetric FOC is applied at 10 s and parameters are correctly estimated at 12 s.

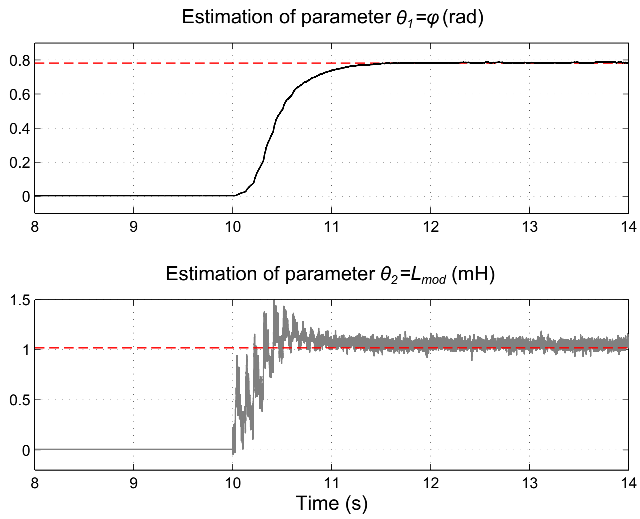

Fig. 6. Estimation of parameters with unscented Kalman filter. Dashed lines are true values of parameters.

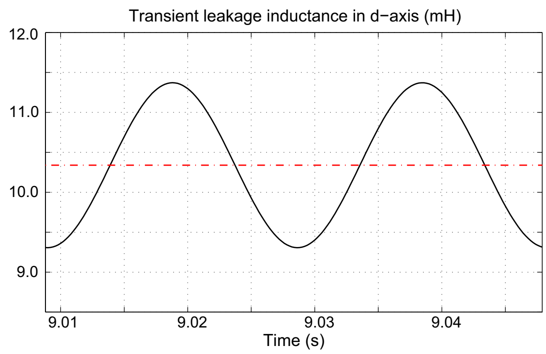

Fig. 7. Complex leakage inductance in d-axis for constant ω_e. Dash-dot line is for the case of symmetric machine.

When the described asymmetric FOC is applied on asymmetric machine as provided with relations (18)-(23) and with correctly estimated parameters, the torque ripple is resolved and significant improvement of system performance is achieved as shown on Fig. 5 after 12 s time.

Fig. 7 shows real part L_{ld} of the asymmetric leakage inductance in the common rotating reference frame defined with (16).

VI. Conclusions

In this paper, an extension of conventional field-oriented control algorithm that achieves smooth operation of asymmetric induction machine is proposed. The method is based on observing changes in the transient leakage inductance and respecting them in the machine control. The proposed approach represents an upgrade of fundamental wave machine model. Detecting changes in the transient leakage inductance is achieved by using an unscented Kalman filter algorithm. Described procedure is applied for the case of stator inter-turn short circuit and provides better system performance than classical field-oriented control. The algorithm is implemented with minimum increase of computational effort and by utilizing already available control structure.

Acknowledgement

The research leading to these results has received funding from the European Community's Seventh Framework Programme under grant agreement no 285939 (ACROSS) and from the European Commission and the Republic of Croatia under grant FP7-SEE-ERA.net PLUS ERA 80/01, project MONGS - Monitoring of Wind Turbine Generator Systems.

References

[1] M. Pacas, "Sensorless Drives in Industrial Applications", *IEEE Industrial Electronics Magazine* vol. 5, no. 2, June 2011, pp. 16-23.

[2] G. Stojičić, P. Nussbaumer, G. Joksimović, M. Vašak, N. Perić and T. M. Wolbank, "Precise Separation of Inherent Induction Machine Asymmetries from Rotor Bar Fault Indicator", *8th IEEE International Symposium on Diagnostics for Electrical Machines, Power Electronics & Drives, SDEMPED*, 2011.

[3] G. Stojičić, G. Joksimović, M. Vašak, N. Perić and T. M. Wolbank, "Increasing Sensitivity of Stator Winding Short Circuit Fault Indicator in Inverter Fed Induction Machines," *15th International Power Electronics and Motion Control Conference, EPE-PEMC ECCE Europe 2012*, Sept. 2012.

[4] A. Yazidi, H. Henao, G. A. Capolino, L. Capocchi, D. Federici, "Double-fed Three-phase Induction Machine Model for Simulation of Inter-turn Short Circuit Fault," *IEEE International Electric Machines and Drives Conference, IEMDC*, pp.571-576, May 2009.

[5] V. Lešić, M. Vašak, N. Perić, G. Joksimović and T. M. Wolbank, "Fault-tolerant Control of a Wind Turbine with a Squirrel-cage Induction Generator and Stator Inter-turn Faults", *The 12th International Workshop on Advanced Motion Control, AMC*, March 2012.

[6] W. Leonhard, *Control of Electrical Drives*, Berlin, Germany: Springer Verlag, ISBN 3-540-41820-2, 2001.

[7] B. K. Bose, *Modern Power Electronics and AC Drives*, Upper Saddle River: Prentice-Hall, ISBN 0-13-016743-6, 2002.

[8] A. H. Bonnet and C. Yung, Increased efficiency versus increased reliability, *IEEE Industry Applications Magazine*, vol.14, no.1, pp.29-36, 2008.

[9] T. M. Wolbank, K. A. Loparo and R. Wöhrnschimmel, "Inverter Statistics for Online Detection of Stator Asymmetries in Inverter-Fed Induction Motors," *IEEE Transactions on Industry Applications*, vol.39, no.4, pp.1102-1108, Jul./Aug. 2003.

[10] H. Oraee, "On-line detection of interturn voltage failures in electrical machine windings," *Proceedings of ICEM 1996*, vol.2, Vigo, Spain, pp.440-445, 1996.

[11] O. Thorsen and M. Dalva, "A survey of faults on induction motors in offshore oil industry, petrochemical industry, gas terminals, and oil refineries," *IEEE Transactions on Industry Applications*, vol.31, pp.1186-1196, Sept./Oct. 1995.

[12] T. M. Wolbank, P. Nussbaumer, Hao Chen and P. E. Macheiner, "Monitoring of Rotor-Bar Defects in Inverter-Fed Induction Machines at Zero Load and Speed," *IEEE Transactions on Industrial Electronics*, vol.58, no.5, pp.1468-1478, May. 2011.

[13] J. Holtz, "Perspectives of Sensorless AC Drive Technology From the State of the Art to Future Trends", *Proc. of the PCIM Europe*, Nürnberg, Germany, pp. 80-87, June 2005.

[14] S.J. Julier and J.K. Uhlmann, *A general method for approximating nonlinear transformations of probability distributions*, Technical report, Dept. of Engineering Science, University of Oxford, November 1996.